A new method to reconstruct radar reflectivities and Doppler information

Liliana Cruz Martin and Gerd Teschke

University of Bremen

P.O.Box 33 04 40

28334 Bremen

January 5, 2004

Abstract

This manuscript is concerned with modeling the measurement process in a multi pulse regime in the context of meteorological radar data processing. Based on the introduced model a method to reconstruct the radar reflectivity and the Doppler information is suggested. In order to show the applicability of the introduced model and of the inversion scheme we present several synthetic test computations.

1 Introduction

In the classical framework a radar device is used in order to transmit electromagnetic waves and to measure backscattered components. Let us assume that the transmitter and receiver are technically combined in one single device. Moreover, assume the following setting: a wave (pulse) is transmitted and after a certain delay (usually the time required for switching between transmitting and receiving) the device starts to sample with a certain rate $1/\delta t$. Each sample represents then a measurement with respect to a certain range. The maximum range R_{max} is given by

$$R_{max} = c \cdot T/2 \quad ,$$

where c is the speed of light, and T the time between transmitting the pulse and measuring/sampling the last value. Usually samples are taken as long as the pulse is traveling through a medium of interest or as long as the power of the backscattered echoes can be measured by the receiver. After time T the next pulse will be transmitted and the measuring process will then be repeated. In this way, the radar device produces time series f_r per range gate r with sampling rate $1/\Delta t = 1/T$. In order to ensure for f_r a certain spectral band width, it is required that T can be chosen adequately small (Nyquist law). But this implies an overlap of echoes of different pulses, i.e. we have ambiguity problems and a decrease of R_{max}. This problem is known as the so-called Range-Doppler-Dilemma.

In principle, the way out must consist of choosing a small pulse repetition time and, in order to ensure R_{max} being adequately large enough, by solving the overlapping problem somehow. Moreover, by the time needed for switching between transmitting and receiving, a small pulse repetition time obviously cause so-called blind ranges (by the switching process, which can technically not be avoided, no measurement corresponding to that range can be taken). To this end, it is suggested to transmit a sequence of pulses in some non-equidistant way. This leads to the fact that blind zones of one pulse can be covered by other pulses.

Roughly speaking, in order to circumvent the Range-Doppler-Dilemma we suggest to introduce a certain type of redundancy in sampling the atmosphere and by applying an algorithm which "de-overlaps" the radar measurement per range gate and generates equidistant (I, Q) - raw data f_r with adequately large sampling rate which is required for ensuring a proper Doppler frequency band width.

The remaining part of the manuscript is organized as follows: in Section 2 we present the new measurement model, in Section 3 we describe how to reconstruct the radar reflectivity and the Doppler information, and, finally, in Section 4 we present several test examples.

The manuscript emphasizes on describing the mathematical idea and not on pointing out the meteorological impact of the invented method. To this end, a detailed meteorological discussion is omitted.

2 Modeling the Measurement Process

In this section, we aim at modeling the measurement process in a multi pulse regime such that the application of an inversion scheme may result in the well-known (I, Q) representation of complex-valued and equidistant raw data f_r (with sampling rate adequately large enough).

In order to model the measurement process of a certain time interval I of length $N\delta t$, we start by choosing a family of L subintervals I_l of length $N_l\delta t$ $(1 \leq l \leq L)$ such that they cover the whole interval I, i.e.

$$\bigcup_{l=1}^{L} I_l = I \ ,$$

and that each I_l contains measurements of all range gates under consideration. We shall see later on that the choice of the position of each I_l corresponds to the sampling points of f_r, i.e. if the I_l's are arranged in an equidistant way, then the f_r's will be reconstructed on an equidistant grid. We remark that is not required that the family of subintervals forms a disjunct partition of I, i.e. the subintervals may overlap, $I_l \cap I_{l'} \neq \emptyset$. We shall also see later on that a certain overlapping causes nice properties of the (I, Q) - data representation f_r.

For our approach the basic assumption is that for each I_l the corresponding reflectivity density distribution P_l is a fixed (complex-valued) function. In our setting P_l depends only on the range gates, i.e. $P_l = P_l(k\delta t)$ with $k = 1, \ldots, K$.

As the next step, we introduce the multi pulse framework. To this end, we define a finite sequence $\{t_m\}_{m=1,\ldots,M}$ which contains the time points in which the cycle of pulses of adequate shapes is transmitted. We assume that $t_m \in I$, for all m, and for simplicity, that $t_m = k_m \delta t$, i.e. the sequence $\{t_m\}$ is determined by a sequence of integers $\{k_m\}_{m=1,\ldots,M}$. Furthermore, we introduce a time gap variable d which represents the small period of time where no sampling can take place (switching process, right after transmitting a pulse), e.g. $d = 3\delta t$.

A reasonable way to represent all informations concerned with the transmitting and the sampling process is to define the pulse-response matrix A^I with respect to I

$$A^I := \begin{pmatrix} \frac{e^{i\phi_1}}{r_1^2} & 0 & \cdots & \cdots & 0 \\ 0 & \ddots & & & \vdots \\ \vdots & 0 & \frac{e^{i\phi_1}}{r_k^2} & & 0 \\ \frac{e^{i\phi_2}}{r_1^2} & & 0 & \ddots & 0 \\ \vdots & \ddots & & 0 & \frac{e^{i\phi_1}}{r_K^2} \\ \frac{e^{i\phi_m}}{r_1^2} & & \frac{e^{i\phi_2}}{r_k^2} & & 0 \\ \vdots & \ddots & & \ddots & 0 \end{pmatrix},$$

where r_k indicates a specific range gate, and $e^{i\phi_m}$ the phase of pulse m. The number of columns of A^I is K, whereas the number of rows corresponds to N.

Now, for each subinterval I_l we extract sub-matrices of A^I which represent the pulse-responses measured in I_l and denote them by A_l, where $\dim(A_l) = K \times N_l$. Incorporating the assumption that P_l is fixed on I_l, we may describe for each time interval I_l the measurement vector Z_l of length N_l by

$$Z_l = A_l P_l + \eta_l \ ,$$

where η_l denotes a certain additive noise model. All these sub-systems can be combined in the following way

$$\mathbf{Z}_\eta = \mathbf{A}\mathbf{P} + \eta \ , \tag{1}$$

where $\mathbf{A}$ is a block-diagonal matrix, i.e.

$$\mathbf{A} = \begin{pmatrix} A_1 & 0 & \dots & 0 \\ 0 & \ddots & & \vdots \\ \vdots & & \ddots & 0 \\ 0 & \dots & 0 & A_L \end{pmatrix} ,$$

and

$$\mathbf{Z} = (Z_1, ..., Z_L)^T \ , \qquad \mathbf{P} = (P_1, ..., P_L)^T \ .$$

If the intervals I_l would not overlap the measurement process would be completely described by the linear model (1). However, in order to improve the flexibility of this model in terms of the sampling frequency of the resulting (I, Q) representation f_r we must incorporate the overlapping. It is obvious that in this case the measurement vector $\mathbf{Z}$ is not the proper representation of the entire measurement process. It becomes necessary to introduce an overlap operator consisting of blocks of diagonal matrices

$$\mathbf{T} =$$

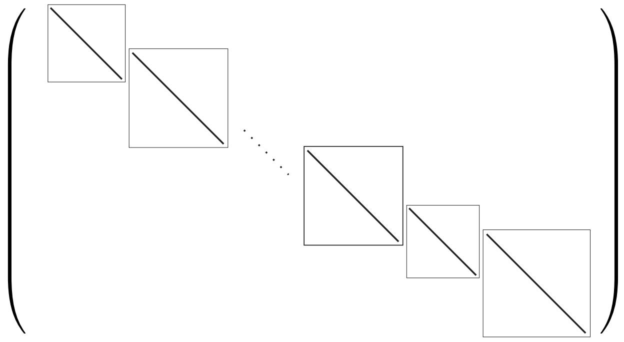

,

where the l-th block is of dimension ${N_l}^2$. The overlap of block l and l' exactly represents the overlap of the subintervals I_l and $I_{l'}$. Hence, the dimension of $\mathbf{T}$ is $\sum_{l=1}^{L} N_l \times N$. Since $\mathbf{T}$ describes the overlap it is reasonable to require that the sum of each row of $\mathbf{T}$ is one. With the help of this operator we can express the general measurement vector denoted by $\hat{\mathbf{Z}}$ as follows

$$\hat{\mathbf{Z}} = \mathbf{TZ} \ ,$$

where the length of $\hat{\mathbf{Z}}$ coincides with the length of I. Defining the operator $\mathbf{B} := \mathbf{TA}$, the final linear measurement model takes the following form

$$\hat{\mathbf{Z}}_\varepsilon = \mathbf{BP} + \varepsilon \ . \tag{2}$$

3 Reflectivity and Doppler Shift Reconstruction

Reconstructing the radar reflectivity and the Doppler information means simply to reconstruct $\mathbf{P}$. This can be formulated as a minimization problem

$$\|\hat{\mathbf{Z}}_\varepsilon - \mathbf{BP}\|_2^2 \longrightarrow \min_{\mathbf{P}} \ .$$

Since (2) is a linear system and assuming that $\mathbf{Cov}(\varepsilon) = \mathbf{W}$, the optimal $\mathbf{P}^*$ is given by

$$\mathbf{P}^* = (\mathbf{B}^T\mathbf{W}^{-1}\mathbf{B})^+\mathbf{W}^{-1}\mathbf{B}^T\hat{\mathbf{Z}}_\varepsilon \ .$$

However, it might be the case that the minimization problem is ill-posed, i.e. the operator $\mathbf{B}$ has no full rank or the condition number of $\mathbf{B}^T\mathbf{W}^{-1}\mathbf{B}$ is quite large. This leads to serious inversion problems. The origins of this deficiency are the sequence $\{t_m\}_{m=1,\dots,M}$ and the overlapping. Thus, a pre-stabilization is given by an adequate choice of the pulse cycle and of the overlapping. The remaining ill-posedness, also induced by the noise term ε, can be reduced by the application of so-called regularization methods, e.g. Tikhonov regularization. The Tikhonov stabilized/regularized solution is computed by minimizing the functional

$$\|\hat{\mathbf{Z}}_\varepsilon - \mathbf{B}\mathbf{P}\|_2^2 + \gamma\|\mathbf{P}\|_2^2 \ ,$$

where the minimizer is given by

$$\mathbf{P}^*_\gamma = (\mathbf{B}^T\mathbf{W}^{-1}\mathbf{B} + \gamma\mathbf{W}^{-1})^{-1}\mathbf{W}^{-1}\mathbf{B}^T\hat{\mathbf{Z}}_\varepsilon \ .$$

In order to choose an adequate regularization parameter γ we could aim at applying Morozov's discrepancy principle. To this end, we have to assume that $\|\epsilon\|_2^2 \leq \mu$. Hence, for an optimal γ we would have

$$\|\hat{\mathbf{Z}}_\varepsilon - \mathbf{B}\mathbf{P}^*_\gamma\|_2^2 \cong \mu \ .$$

To find numerically a proper γ we choose $c, \gamma_0 > 0$, some q with $0 < q < 1$, and define a sequence $\gamma_j := q^j\gamma_0$. Then, the iterative method to determine an adequate

γ goes as follows: compute $P^*_{\gamma_j}$ until

$$\mu \leq \|\hat{\mathbf{Z}}_\varepsilon - \mathbf{T}\mathbf{P}^*_{\gamma_j}\|_2^2 \leq c\mu$$

holds.

We finally remark that there exist of course other ways to solve the minimization problem (2). However, here we just have suggested one suitable way to reconstruct $\mathbf{P}$.

4 Numerical Simulations

For our first synthetic test example we have chosen the following setting: length of sampling interval I is $1050\delta t$; length of I_l is $250\delta t$ with overlaps of $50\delta t$, i.e. $L = 5$. We note that L determines the resulting sampling rate of the (I, Q) - data representation f_r per range gate r. Furthermore, we introduce the time gap variable d which is chosen to be $5\delta t$. The sequence $\{t_m\}$ is determined by the following sequence of integers {0, 70, 90, 120, 170, 180, 210, 250, 320, 340, 370, 420, 430, 460, 500, 570, 590, 620, 670, 680, 710, 750, 820, 840, 870, 920, 930, 960}. Assuming we sample at 120 ($= K$) range gates, the resulting matrix A^I, the corresponding submatrices A_l, and the final model matrix $\mathbf{B}$ are of the form as displayed in Figures 1 and 2.

In order to generate synthetic data we assume a very simple model for the reflectivity functions P_l, namely

$$P_l(k\delta t) = e^{-\frac{(1.001\cdot l\cdot k\delta t-(50+10\cdot l))^2}{1000}} \cdot e^{i\frac{3k\delta t}{L}} \;, \quad 1 \leq l \leq L \;, \quad 1 \leq k \leq K \;,$$

see Figure 3. The simulated measurements are obtained by adding i.i. standard normal d. noise ε, see model (2), i.e.

$$\hat{\mathbf{Z}}_\varepsilon = \mathbf{BP} + c \cdot \varepsilon \ , \quad \text{with} \quad c = 0.001,\ 0.0015,\ 0.003\ .$$

To find reasonable reflectivity functions $\mathbf{P}^*$ (and therewith the Doppler information), we apply the Tikhonov regularization method with $\gamma = 0.000001$. The results are displayed is Figure 4.

In order to show how to obtain (I, Q) - data series f_r with higher sampling rate (two times higher that in the previous example) we present another example where we have used the same setting but now with $L = 10$, see Figures 7, 8, 9, and 10.

In both examples we observe that the complex-valued reflectivity function can be reconstructed. In the presence of noise we may see that the reconstruction becomes coarser as larger the range gate is. This depends clearly on the signal to noise ratio of the received echoes (since the energy decreases with $\sim 1/r_k^2$). To obtain optimal results one has to find the right balance between the choice of the pulse cycle, the overlapping, the influence of noise, and the parameters of the inversion scheme.

5 Conclusion

In this manuscript we have presented a model which allows to overcome the Range-Doppler-Dilemma. The invented method is based on a non-equidistant multi pulse regime and is a combination of linear modeling and a overlapping process which ensures an adequate Doppler frequency band width of the resulting (I, Q) - data series f_r per range gate. The suggest reconstruction scheme is based Tikhonov regularization. In order to improve the accuracy and to reduce the computational cost one may use more sophisticated inversion schemes.

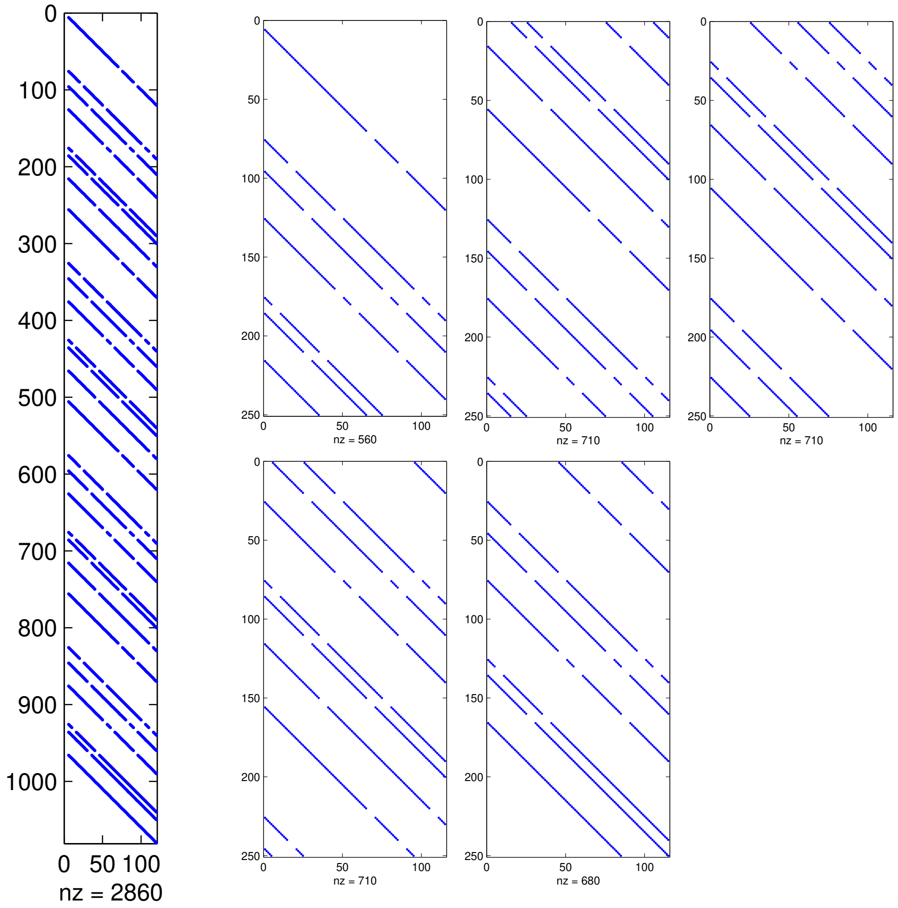

Figure 1: Left: the total pulse response matrix A, right: the five sub-matrices A_l.

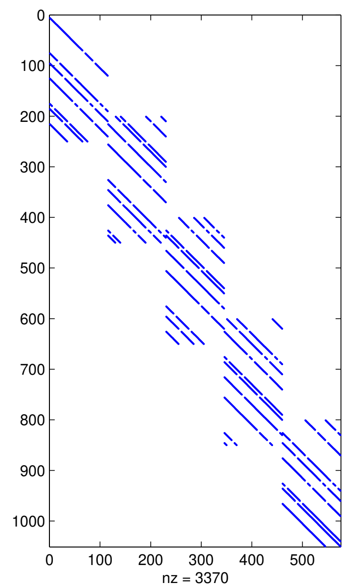

Figure 2: The final model matrix $\mathbf{B}$.

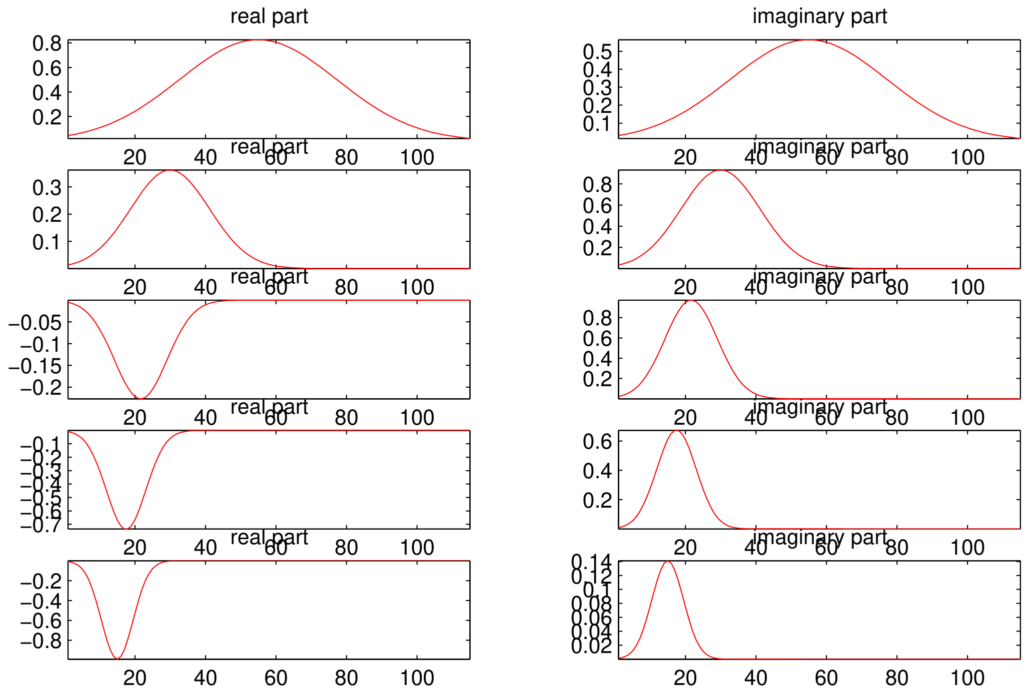

Figure 3: The simulated reflectivity functions P_l, $l = 1$ (top), $\ldots, 5$ (down).

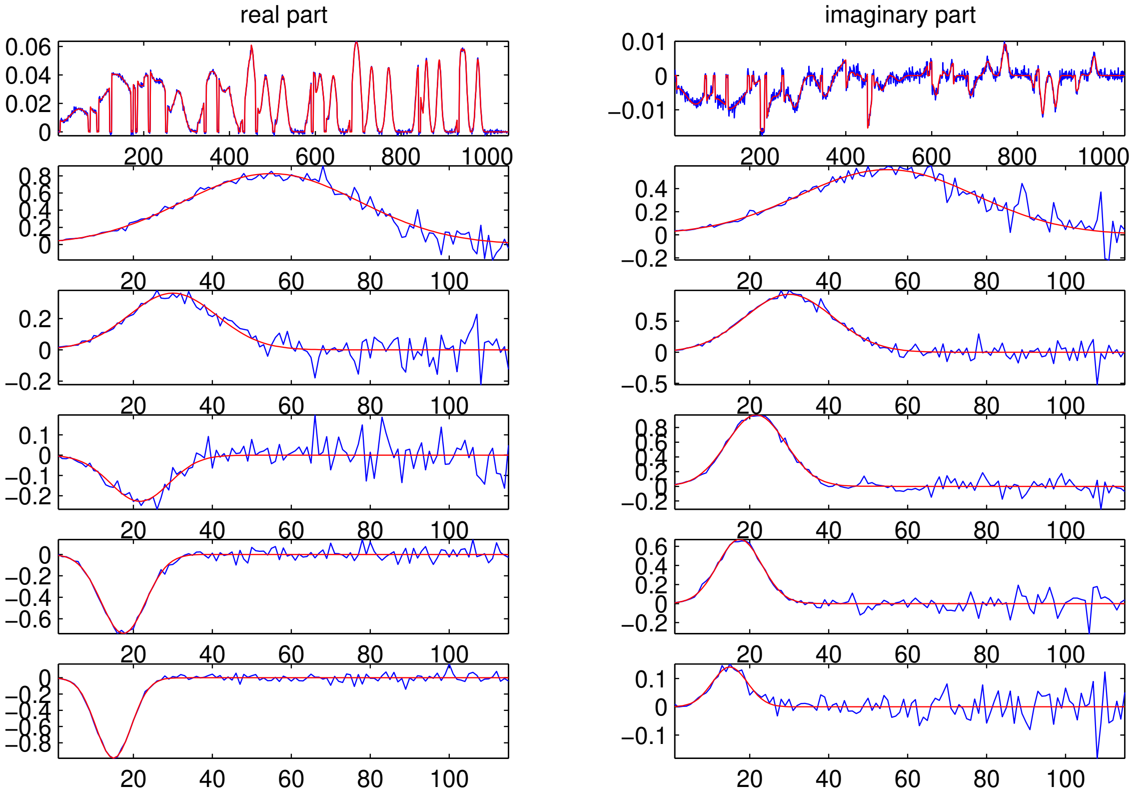

Figure 4: The first row shows the simulated $\hat{\mathbf{Z}}_\varepsilon$ (red without noise). The remaining rows show the Tikhonov reconstructions of P_l, with $c = 0.001$, $l = 1$ (top), $\ldots, 5$ (down).

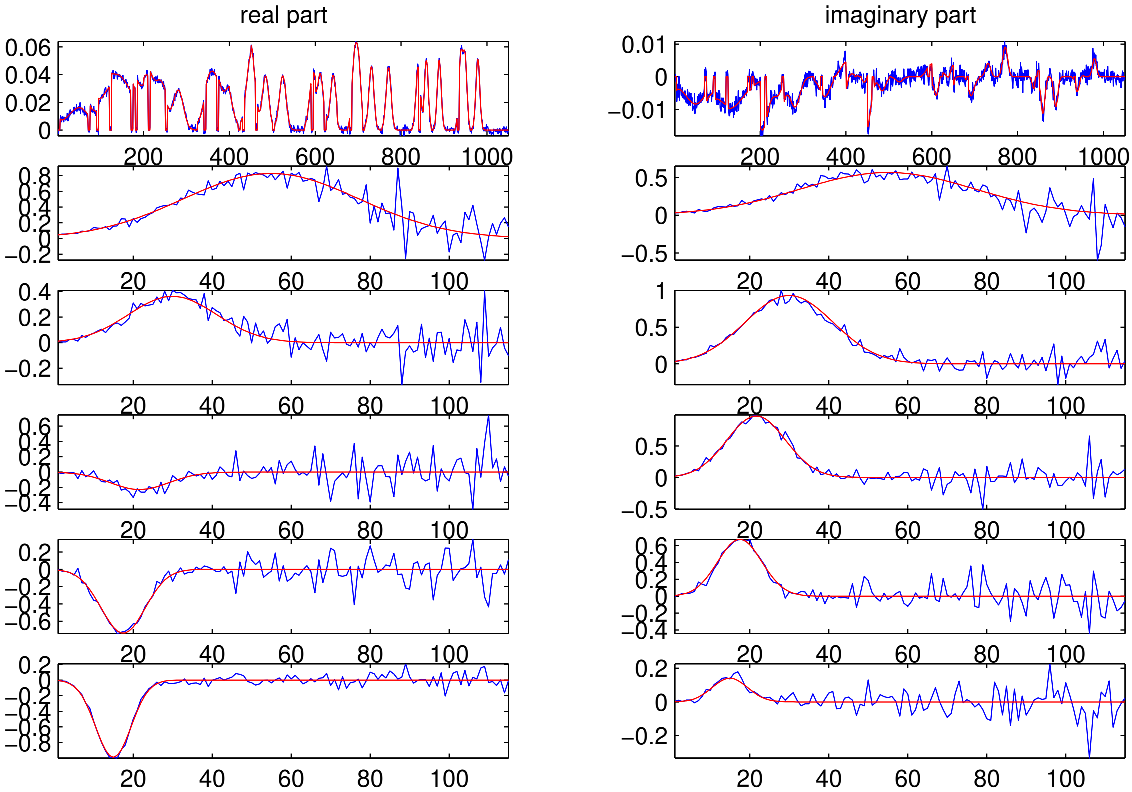

Figure 5: The first row shows the simulated $\hat{\mathbf{Z}}_\varepsilon$ (red without noise). The remaining rows show the Tikhonov reconstructions of P_l, with $c = 0.0015$, $l = 1$ (top), $\ldots, 5$ (down).

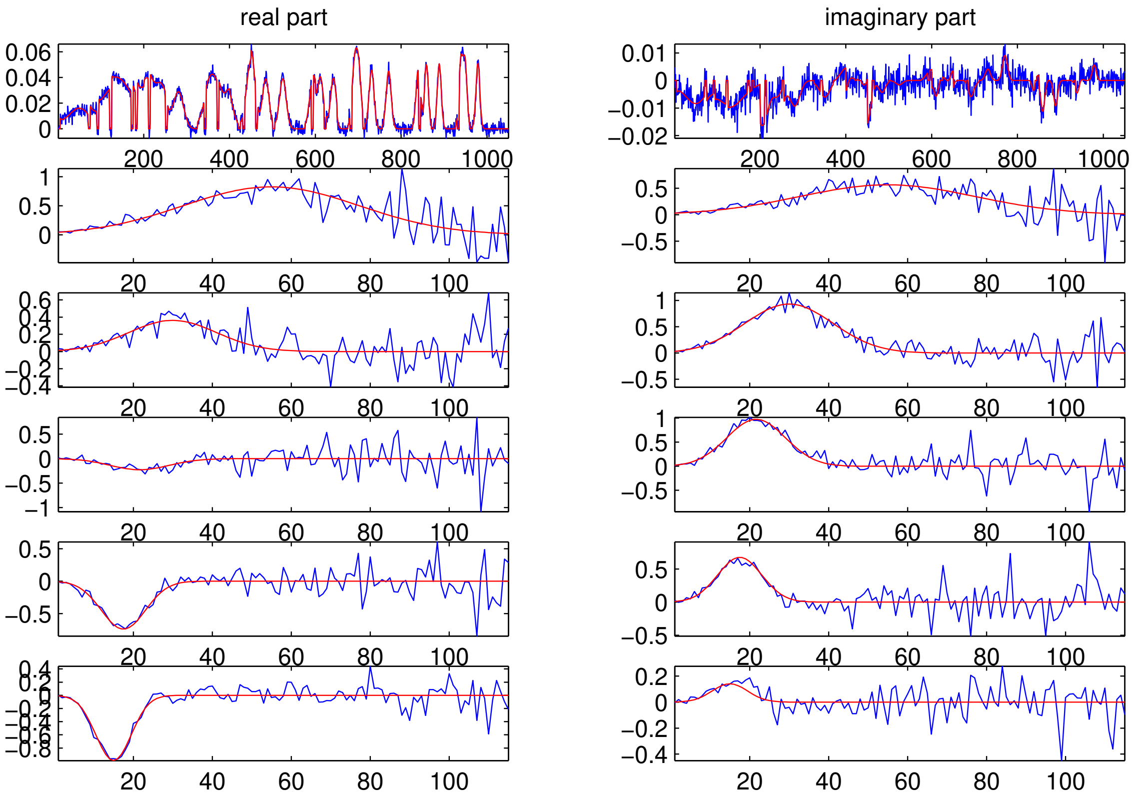

Figure 6: The first row shows the simulated $\hat{\mathbf{Z}}_\varepsilon$ (red without noise). The remaining rows show the Tikhonov reconstructions of P_l, with $c = 0.003$, $l = 1$ (top), $\ldots, 5$ (down).

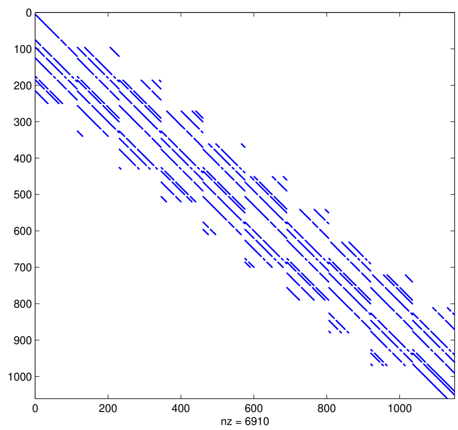

Figure 7: Matrix $\mathbf{B}$ ($L = 10$).

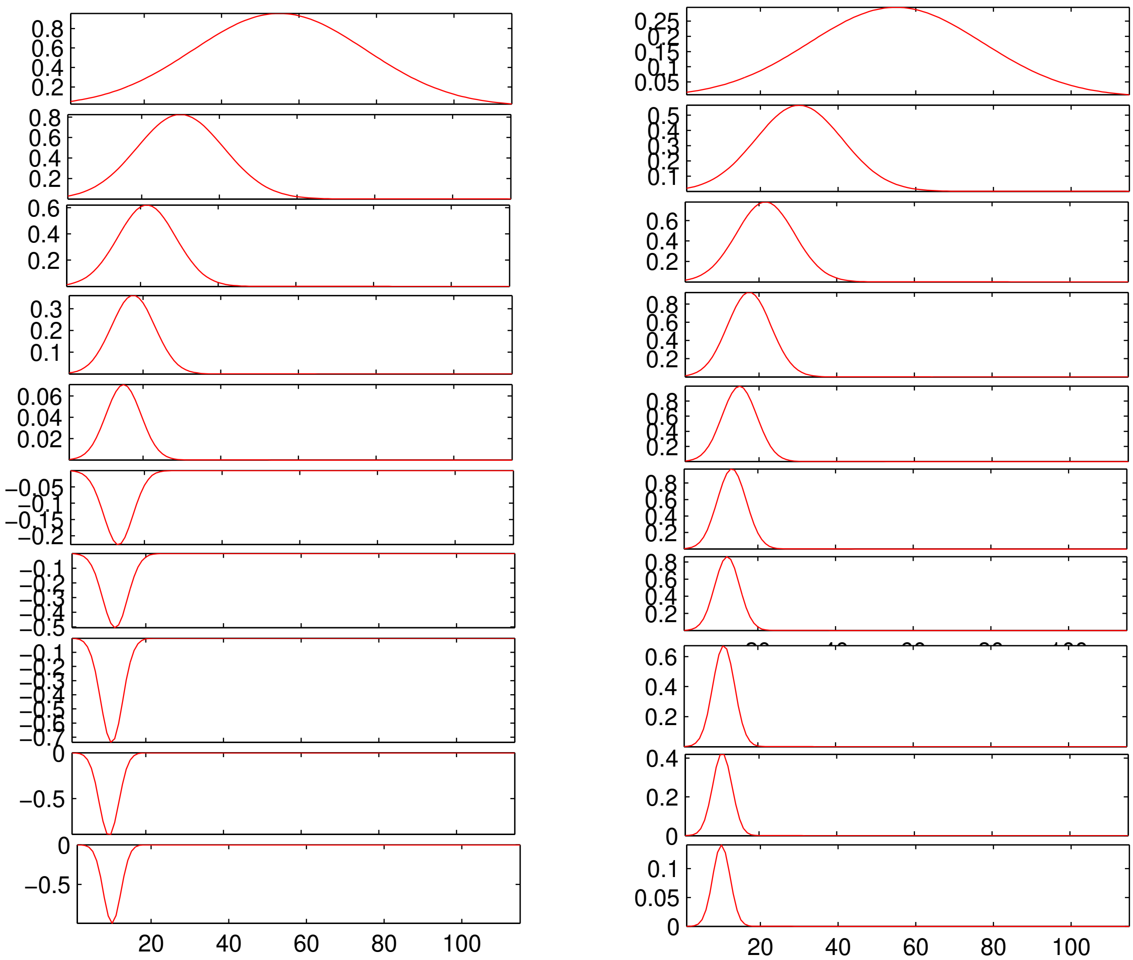

Figure 8: The simulated reflectivity functions P_l, $l = 1$ (top), $\ldots, 10$ (down).

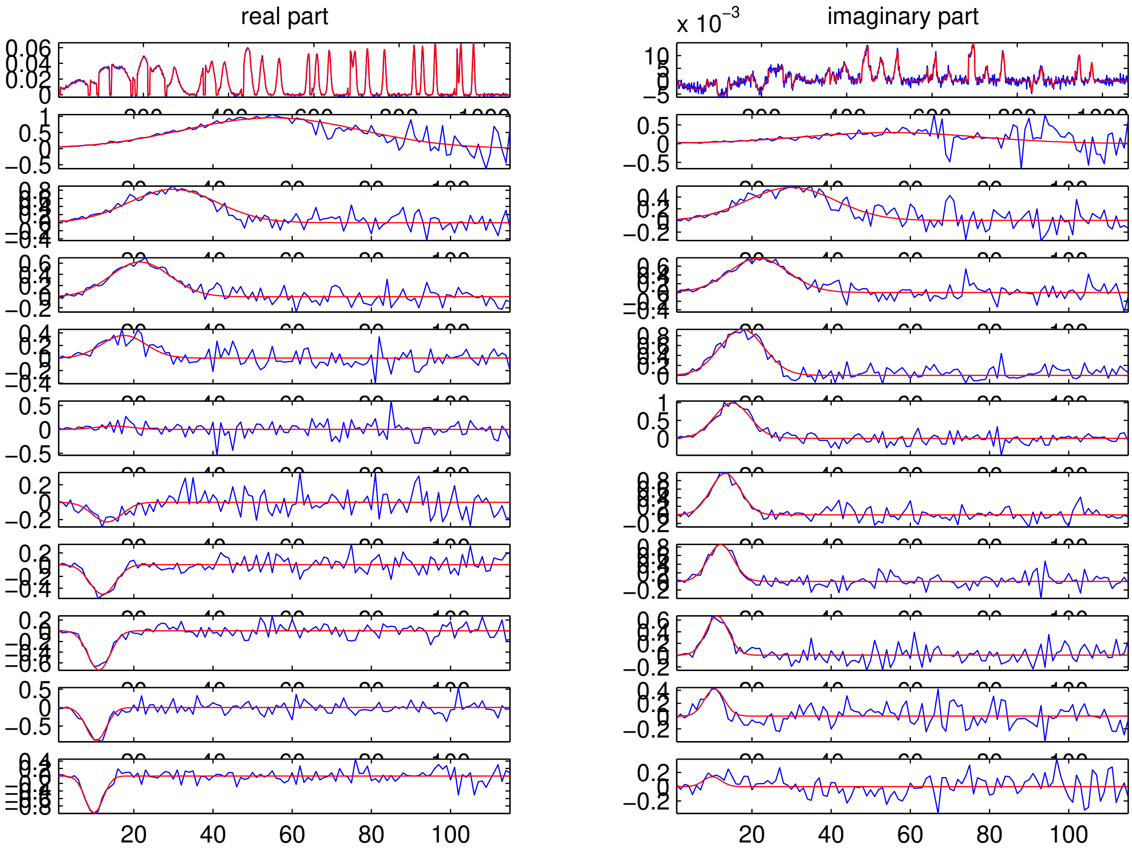

Figure 9: The first row shows the simulated $\hat{\mathbf{Z}}_\varepsilon$ (red without noise). The remaining rows show the Tikhonov reconstructions of P_l, with $c = 0.001$, $l = 1$ (top), $\ldots, 10$ (down).

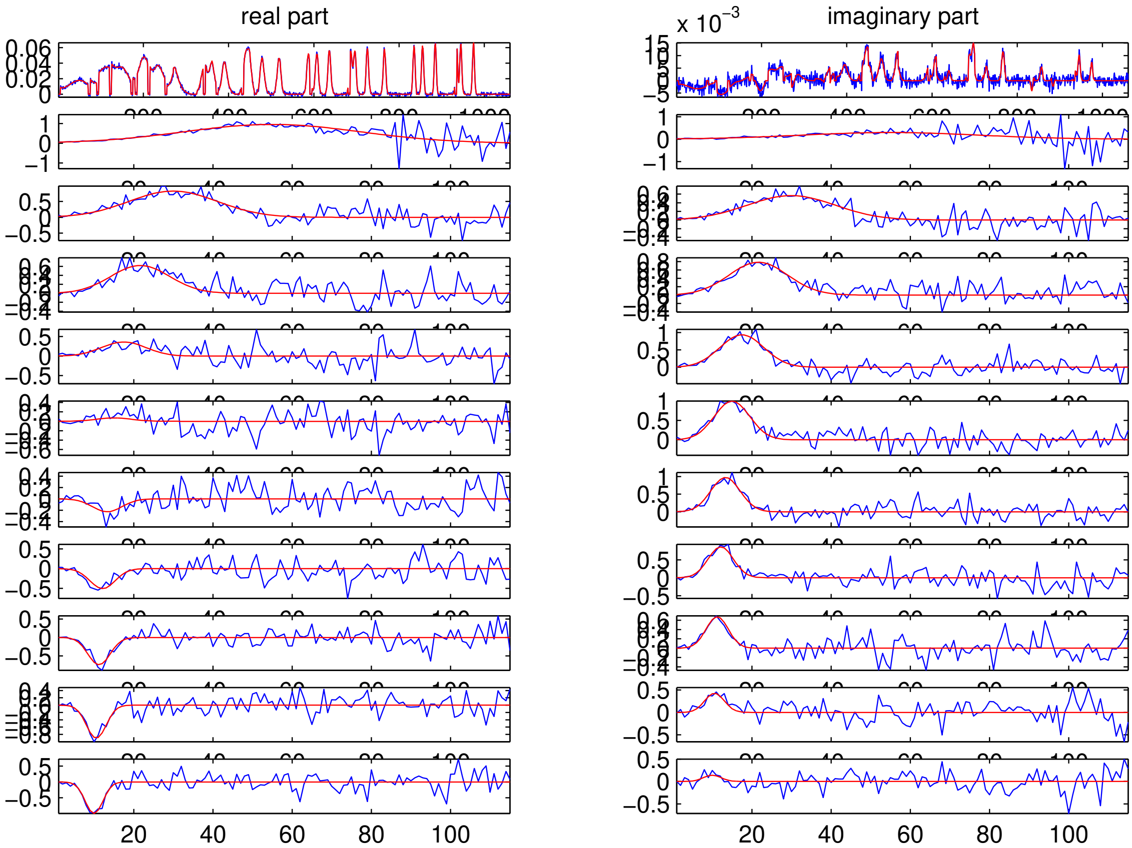

Figure 10: The first row shows the simulated $\hat{\mathbf{Z}}_\varepsilon$ (red without noise). The remaining rows show the Tikhonov reconstructions of P_l, with $c = 0.0015$, $l = 1$ (top), $\ldots$, 10 (down).